Glycogen Synthase Kinase 3 Regulates *N*-Methyl-D-aspartate Receptor Channel Trafficking and Function in Cortical Neurons

Paul Chen, Zhenglin Gu, Wenhua Liu, and Zhen Yan

Department of Physiology and Biophysics, State University of New York at Buffalo, School of Medicine and Biomedical Sciences, Buffalo, New York

ABSTRACT

Emerging evidence has suggested that glycogen synthase kinase 3 (GSK-3) is a key regulatory kinase involved in a plethora of processes in the nervous system, including neuronal development, mood stabilization, and neurodegeneration. However, the cellular mechanisms underlying the actions of GSK-3 remain to be identified. In this study, we examined the impact of GSK-3 on the *N*-methyl-D-aspartate (NMDA) receptor channel, a central player involved in cognitive and emotional processes. We found that application of various structurally different GSK-3 inhibitors caused a long-lasting reduction of NMDA receptor-mediated ionic and synaptic current in cortical pyramidal neurons. Cellular knockdown of GSK-3β in neuronal cultures with a small interfering RNA led to smaller NMDA receptor current and loss of its regulation by GSK-3 inhibitors. The NR2B subunit-containing NMDA receptor was the primary target of GSK-3, but the GSK-3 modulation of NMDAR current did not involve the motor protein kinesin superfamily member 17-based transport of NR2B-containing vesicles along microtubules. Combined electrophysiological, immunocytochemical, and biochemical evidence indicated that GSK-3 inhibitors induced the down-regulation of NMDAR current through increasing the Rab5-mediated and PSD-95-regulated NMDAR internalization in a clathrin/dynamin-dependent manner.

Glycogen synthase kinase 3 (GSK-3) was initially identified as an enzyme that regulates glycogen synthesis in response to insulin (Welsh et al., 1996). Two distinct but closely related GSK-3 forms, GSK-3α and GSK-3β, have been discovered. GSK-3, which is usually active in resting cells, is a critical downstream element of the phosphoinositide 3-kinase/Akt pathway, and its activity can be inhibited by Akt-mediated phosphorylation at serine residues (Ser21 for GSK-3α and Ser9 for GSK-3β) on their N-terminal domain (Cross et al., 1995). Recently GSK-3 has emerged as a multifunctional serine/threonine kinase involved in many cellular processes (Frame and Cohen, 2001), and pharmacological inhibitors of GSK-3 offer great potential for the treatment of a variety of disorders (Meijer et al., 2004). Considerable studies have shown that GSK-3β is a crucial player in regulating axon growth and neuronal polarity during development (Zhou and Snider, 2005). GSK-3 has also been implicated in the pathogenesis of mood disorders (Coyle and Duman, 2003), because it is one of the main targets of lithium (Phiel and Klein, 2001), the most established treatment for manic-depression illness. Moreover, GSK-3 is proposed as an important mediator of dopamine actions in vivo (Beaulieu et al., 2004), and converging evidence suggests that impaired Akt/GSK-3β signaling contributes to schizophrenia (Emamian et al., 2004). In addition, GSK-3 is a potential target of Alzheimer's disease (AD), because inhibition of GSK-3 reduces the production of Aβ peptides in amyloid plaques (Phiel et al., 2003) and the hyperphosphorylation of τ protein in neurofibrillary tangles (Hong et al., 1997), two pathological hallmarks of AD.

To understand the cellular mechanisms underlying the broad physiological effects of GSK-3, it is essential to identify the molecular targets of GSK-3. The NMDA glutamate receptor, a principal subtype of excitatory ligand-gated ion channel, has been implicated in multiple neuronal functions

ABBREVIATIONS: GSK-3, glycogen synthase kinase-3; AD, Alzheimer's disease; NMDA, *N*-methyl-D-aspartate; NR2A, *N*-methyl-D-aspartate receptor subunit 2A; NR2B, *N*-methyl-D-aspartate receptor subunit 2B; KIF17, kinesin superfamily member 17; TDZD, 4-benzyl-2-methyl-1,2,4-thiadiazolidine-3,5-dione; NMDAR, *N*-methyl-D-aspartate receptor; BAPTA, 1,2-bis(2-aminophenoxy)ethane-*N*,*N*,*N'*,*N'*-tetraacetic acid; DMSO, dimethyl sulfoxide; ANOVA, analysis of variance; DIV, days in vitro; GFP, green fluorescent protein; siRNA, small interfering RNA; EPSC, excitatory postsynaptic current; DN, dominant negative; CA, constitutively active; AP, activator protein; QX-314, 2-((2,6-dimethylphenyl)amino)-*N*,*N*,*N*-triethyl-2-oxoethanaminium; SB216763, 3-(2,4-dichlorophenyl)-4-(1-methyl-1*H*-indol-3-yl)-1*H*-pyrrole-2,5-dione.

ranging from synapse formation, synaptic plasticity, learning, and memory, to mental disorders (Tsai and Coyle, 2002) and Alzheimer's disease (Selkoe, 2002). It prompts us to hypothesize that one important target of GSK-3 could be the NMDA receptor. To test this, we examined the impact of GSK-3 on NMDA receptor function in cortical pyramidal neurons. We found that inhibiting GSK-3 activity suppresses NMDAR current through a mechanism involving the NMDAR internalization.

Materials and Methods

Whole-Cell Recordings. Acutely dissociated frontal cortical pyramidal neurons from young adult (3–5 weeks postnatal) Sprague-Dawley rats or cortical cultures from 18-day rat embryos were prepared using procedures described previously (Wang et al., 2003). Recordings of whole-cell ion channel current used standard voltage-clamp techniques (Yuen et al., 2005a). The internal solution consisted of 180 mM N-methyl-D-glucamine, 40 mM HEPES, 4 mM $MgCl_2$, 0.1 mM BAPTA, 12 mM phosphocreatine, 3 mM Na_2ATP, 0.5 mM Na_2GTP, and 0.1 mM leupeptin, pH 7.2 to 7.3, 265 to 270 mOsM. The external solution consisted of 127 mM NaCl, 20 mM CsCl, 10 mM HEPES, 1 mM $CaCl_2$, 5 mM $BaCl_2$, 12 mM glucose, 0.001 mM tetrodotoxin, and 0.02 mM glycine, pH 7.3 to 7.4, 300–305 mOsM. Recordings were obtained with an Axon Instruments 200B patch clamp amplifier that was controlled and monitored with an IBM PC running pCLAMP (version 8) with a DigiData 1320 series interface (Molecular Devices, Sunnyvale, CA). Electrode resistances were typically 2 to 4 $M\Omega$ in the bath. After seal rupture, series resistance (4–10 $M\Omega$) was compensated (70–90%) and periodically monitored. The cell membrane potential was held at −60 mV. The application of NMDA (100 μM) evoked a partially desensitizing inward current that could be blocked by the NMDA receptor antagonist D-2-amino-5-phosphonovalerate (50 μM). NMDA was applied for 2 s every 30 s to minimize desensitization-induced decrease of current amplitude. Drugs were applied with a gravity-fed "sewer pipe" system. The array of application capillaries (approximately 150 μm internal diameter) was positioned a few hundred micrometers from the cell under study. Solution changes were effected by the SF-77B fast-step solution stimulus delivery device (Warner Instruments, Hamden, CT).

GSK-3 inhibitors 4-benzyl-2-methyl-1,2,4-thiadiazolidine-3,5-dione (TDZD; Calbiochem, San Diego, CA), SB216763 (Tocris, Ellisville, MO), α-4-dibromoacetophenone (Calbiochem), and phosphatase inhibitors okadaic acid, its inactive analog okadaic acid methyl ester, and microcystin (Calbiochem) were made up as concentrated stocks in DMSO or water and stored at −20°C. Stocks were thawed and diluted immediately before use. The amino acid sequence for the dynamin inhibitory peptide is QVPSRPNRAP. The polyclonal anti-Rab5 antibody (Santa Cruz Biotechnology, Santa Cruz, CA) was raised against the full-length human Rab5A.

Data analyses were performed with AxoGraph (Molecular Devices), Kaleidagraph (Abelbeck/Synergy Software, Reading, PA), Origin 6 (OriginLab Corp, Northampton, MA) and Statview (SAS Institute, Cary, NC). For analysis of statistical significance, Mann-Whitney U tests were performed to compare the current amplitudes in the presence or absence of GSK-3 inhibitors. ANOVA tests were performed to compare the differential degrees of current modulation between groups subjected to different treatment.

Electrophysiological Recordings in Slices. To evaluate the regulation of NMDAR-mediated excitatory postsynaptic current in cortical slices, the whole-cell voltage-clamp recording technique was used (Wang et al., 2003; Yuen et al., 2005a). Electrodes (5–9 $M\Omega$) were filled with the following internal solution: 130 mM cesium-methanesulfonate, 10 mM CsCl, 4 mM NaCl, 10 mM HEPES, 1 mM $MgCl_2$, 5 mM EGTA, 2.2 mM QX-314, 12 mM phosphocreatine, 5 mM

MgATP, 0.2 mM Na_3GTP, and 0.1 mM leupeptin, pH 7.2 to 7.3, 265 to 270 mOsM. The slice (300 μm) was placed in a perfusion chamber attached to the fixed-stage of an upright microscope (Olympus, Tokyo, Japan) and submerged in continuously flowing oxygenated artificial cerebrospinal fluid containing 6-cyano-2,3-dihydroxy-7-nitroquinoxaline (20 μM) and bicuculline (10 μM) to block α-amino-3-hydroxy-5-methyl-4-isoxazolepropionic acid/kainate receptors and $GABA_A$ receptors. Cells were visualized with a 40× water-immersion lens and illuminated with near infrared light, and the image was detected with an infrared-sensitive charge-coupled device camera. A Multiclamp 700A amplifier was used for these recordings. Tight seals (2–10 $G\Omega$) from visualized pyramidal neurons were obtained by applying negative pressure. The membrane was disrupted with additional suction, and the whole-cell configuration was obtained. The access resistances ranged from 13 to 18 $M\Omega$ and were compensated 50 to 70%. Evoked currents were generated with a 50-μs pulse from a stimulation isolation unit controlled by an S48 pulse generator (Astro-Med, West Warwick, RI). A bipolar stimulating electrode (FHC) was positioned ~100 μm from the neuron under recording. Before stimulation, cells (voltage-clamped at −70 mV) were depolarized to +60 mV for 3 s to fully relieve the voltage-dependent Mg^{2+} block of NMDAR channels. Clampfit software (Molecular Devices) was used to analyze evoked synaptic activity.

Biochemical Measurement of Surface-Expressed Receptors. The surface NMDA receptors were detected as described previously (Wang et al., 2003). In brief, after treatment, cortical slices were incubated with artificial cerebrospinal fluid containing 1 mg/ml sulfo-N-hydroxysuccinimide-LC-Biotin (Pierce Chemical Co., Rockford, IL) for 20 min on ice. The slices were then rinsed three times in Tris-buffered saline to quench the biotin reaction, followed by homogenization in 300 μl of modified radioimmunoprecipitation assay buffer (1% Triton X-100, 0.1% SDS, 0.5% deoxycholic acid, 50 mM $NaPO_4$, 150 mM NaCl, 2 mM EDTA, 50 mM NaF, 10 mM sodium pyrophosphate, 1 mM sodium orthovanadate, 1 mM phenylmethylsulfonyl fluoride, and 1 mg/ml leupeptin). The homogenates were centrifuged at 14,000g for 15 min at 4°C. Protein (15 μg) was removed to measure total NR1. For surface protein, 150 μg of protein was incubated with 100 μl of 50% Neutravidin Agarose (Pierce Chemical Co.) for 2 h at 4°C, and bound proteins were resuspended in 25 μl of SDS sample buffer and boiled. Quantitative Western blots were performed on both total and biotinylated (surface) proteins using anti-NR1 (1:1000; Upstate Biotechnology, Lake Placid, NY).

Immunocytochemistry. Cultured cortical neurons (12–15 DIV) were used for immunocytochemical experiments. NR2B or NR2A tagged with GFP at the extracellular N terminus (Luo et al., 2002) was used to transfect cortical cultures. For the detection of GFP-NR2B or GFP-NR2A on the cell surface, cultured neurons (48 h after transfection) were treated with different agents, and then they were fixed in 4% paraformaldehyde but were not permeabilized. After background blocking in bovine serum albumin, the cells were incubated with the anti-GFP antibody (1:100; Chemicon International, Temecula, CA) at room temperature for 1 h. After washing off the primary antibodies, the cells were incubated with a rhodamine-conjugated secondary antibody (1:200; Sigma, St. Louis, MO) for 50 min at room temperature. After washing in phosphate-buffered saline three times, the coverslips were mounted on slides with Vectashield mounting media (Vector Laboratories, Inc., Burlingame, CA).

Labeled cells were imaged using a 40× or 100× objective with a cooled charge-coupled device camera mounted on a Nikon microscope (Nikon, Tokyo, Japan). All specimens were imaged under identical conditions and analyzed using identical parameters. Images were first subtracted from the average background fluorescence with a threshold, and then the level of surface NMDAR immunoreactivity on the same length of dendrites in treated versus untreated cells was compared. Three to five independent experiments were performed. On each coverslip, the immunofluorescence intensity of five to eight neurons was quantified. For each neuron, the immunoreactivity of four neurites (100 μm each, with similar diameters and distances

from the soma) was measured. Quantitative analyses were conducted blindly (without knowledge of experimental treatment).

Small Interfering RNA and Antisense. To suppress the expression of GSK-3 in cultured neurons, we used the small interfering RNA (siRNA), a potent agent for sequence-specific gene silencing. The GSK-3 siRNA oligonucleotide sequences (Phiel et al., 2003) selected from GSK-3α mRNA were the following: 5′-UUCUACUCC-AGUGGUGAGAdTdT-3′ (sense) and 5′-UCUCACCACUGG-AGUA-GAAdT dT-3′ (antisense); and from GSK-3β mRNA, 5′-AUCUUUG-GAGCCACU-GAUUdTdT-3′ (sense) and 5′- AAUCAGUGGCUCCA-AAGAUdTdT-3′ (antisense). siRNA was synthesized (Ambion, Austin, TX) and cotransfected with enhanced GFP into cultured cortical neurons (11 DIV) using the Lipofectamine 2000 method. Two to 3 days after transfection, electrophysiological recordings were performed. To test the effectiveness of GSK-3α/β siRNAs, immunocytochemical experiments were performed as described previously (Yuen et al., 2005a) with antibodies against GSK-3α or GSK-3β (1:100; Cell Signaling Technology).

To knock down the expression of KIF17 in cultured cortical neurons, we used the antisense oligonucleotide approach as described previously (Yuen et al., 2005a). The antisense oligonucleotide against KIF17 cDNA was 5′-CAGAGGCTCACCACCGAA-3′, and the corresponding sense oligonucleotide was 5′-TTCGGTGGTGAGC-CTCTG-3′. After 8 to 11 days of culture, a 1 μM concentration of oligonucleotides was added directly to the culture medium. Two to 3 days after being exposed to these oligonucleotides, electrophysiological recordings were performed on the cultured neurons.

Cloning, Expression, and Purification of Proteins. Wild-type Rab5 cDNA was cloned by reverse transcription-polymerase chain reaction using mouse brain total RNA. After sequence verification, the cDNA was subcloned into the bacterial expression vector pQE-80 (QIAGEN, Valencia, CA), which added a His$_6$ tag at the N terminus of the protein. Rab5 mutants (S34N and Q79L) were generated by site-directed mutagenesis using the QuikChange Kit from Stratagene (La Jolla, CA). Rab5 expression in the M15 strain of *Escherichia coli* (QIAGEN) was induced by adding isopropyl β-D-thiogalactoside to 1 mM final concentration for 4 to 5 h at 25°C (to minimize the formation of inclusion bodies). Rab5 in cleared *E. coli* lysate was purified by affinity chromatography using the His Gravitrap column (GE Healthcare, Chalfont St. Giles, Busckinghamshire, UK) according to the manufacturer's protocol. His$_6$-tagged Rab5 proteins were eluted from the column in a buffer containing 50 mM Tris, 500 mM NaCl, and 300 mM imidazole, pH 7.4. Fractions of eluate were analyzed by SDS-polyacrylamide gel electrophoresis and Coomassie Blue staining to identify the peak fractions containing Rab5 proteins. Western blotting with the polyclonal anti-Rab5 antibody (Santa Cruz Biotechnology) was also performed to verify the expression of purified Rab5 protein. The most pure one or two fractions (shown as a single band by Coomassie blue staining) were dialyzed against phosphate-buffered saline before being used in electrophysiological experiments.

Western Blot and Coimmunoprecipitation. Western blotting procedures were similar to what was described previously (Gu et al., 2005). The phospho-GSK-3α/β (Ser21/9) antibody (1:1000; Cell Signaling Technology) was used to detect inactivated GSK-3. For coimmunoprecipitation experiments, after treatment with indicated agents, each slice was collected and homogenized in 1 ml of lysis buffer (50 mM Tris, 1% deoxycholic acid, 10 mM EDTA, 10 mM EGTA, 1 mM phenylmethylsulfonyl fluoride, and 1 mg/ml leupeptin). Lysates were ultracentrifuged (200,000g) at 4°C for 60 min. Supernatant fractions were incubated with an anti-NR1 antibody (2 μg; Upstate Biotechnology) for 1 h at 4°C, followed by incubation with 50 μl of protein A/G plus agarose (Santa Cruz Biotechnology) for 1 h at 4°C. Immunoprecipitates were washed three times with lysis buffer containing 0.2 M NaCl, then boiled in 2× SDS loading buffer for 5 min, and separated on 7.5% SDS-polyacrylamide gels. Western blotting experiments were performed with an anti-PSD-95 antibody (1:1000; Affinity BioReagents, Golden, CO).

Results

GSK-3 Inhibitors Reduce NMDAR-Mediated Current in Cortical Pyramidal Neurons. Because GSK-3 has a high basal activity and signaling pathways often proceed by inhibiting GSK-3 activity (Doble and Woodgett, 2003), we first examined the effect of GSK-3 inhibitors on NMDA receptor-mediated current in dissociated cortical pyramidal neurons to determine the potential influence of GSK-3 on NMDA receptors. Application of TDZD (10 μM), a highly selective non–ATP-competitive inhibitor of GSK-3, caused a potent reduction in the amplitude of NMDA (100 μM)-evoked current, whereas the NMDAR current amplitude was stable throughout the recording period with application of the control vehicle DMSO. The time courses and current traces from representative cells are shown in Fig. 1A. Dose-response experiments (Fig. 1B) indicated that different concentrations of TDZD inhibited NMDR current to different extents with the EC$_{50}$ ~1.7 μM.

To verify the effect of GSK-3 on NMDA receptor current, we further examined other structurally different GSK-3 inhibitors. As shown in Fig. 1C, SB216763 (10 μM), another potent and selective GSK-3 inhibitor, produced a strong reduction of NMDAR current in the dissociated cortical neuron. Application of LiCl (5 mM), a known inhibitor of GSK-3 in vitro and in neurons (Phiel and Klein, 2001), also potently suppressed NMDAR current (Fig. 1D). The effect of different GSK-3 inhibitors on NMDAR current is summarized in Fig. 1E. TDZD had a significant inhibitory effect on the peak NMDAR current amplitude in freshly isolated cortical pyramidal neurons (22.0 $\pm$ 1.1%, $n = 31$, $p < 0.001$, Mann-Whitney). TDZD also inhibited the steady-state NMDAR current amplitude (19.3 $\pm$ 1.0%, $n = 10$, $p < 0.001$, Mann-Whitney). Fitting the NMDAR current with a single exponential equation indicated that TDZD did not significantly alter the desensitization profile of NMDAR current (τ in control: 0.60 $\pm$ 0.05 s; τ in TDZD: 0.59 $\pm$ 0.03 s, $n = 5$). Similar to the effect of TDZD, other GSK-3 inhibitors, including SB216763, dibromoacetophenone (15 μM), LiCl, and Li$_2$CO$_3$ (1 mM), also significantly suppressed peak NMDAR current amplitude (SB216763: 21.0 $\pm$ 1.0%, $n = 10$; dibromoacetophenone: 18.7 $\pm$ 3.0%, $n = 9$; LiCl: 19.7 $\pm$ 2.0%, $n = 13$; Li$_2$CO$_3$: 19.5 $\pm$ 6.0%, $n = 8$). Similar effects were found in cultured cortical pyramidal neurons with TDZD or LiCl (TDZD: 17.3 $\pm$ 2.1%, $n = 20$; LiCl: 19.4 $\pm$ 3.0%, $n = 6$, $p < 0.001$, Mann-Whitney).

The reduction of NMDAR current induced by all of these GSK-3 inhibitors was robust and irreversible after 10 to 15 min of washing. Partial (40–50%) or near complete (70–80%) recovery could happen with shorter application of GSK-3 inhibitors and more prolonged washing ($n = 6$, data not shown). It suggests that persistent inhibition of GSK-3 could produce a long-lasting effect on NMDA receptors.

GSK-3α and GSK-3β are inactivated through phosphorylation of serine residues (Ser21 for GSK-3α and Ser9 for GSK-3β) on their N-terminal domain (Cross et al., 1995; Frame and Cohen, 2001), so we used an antibody selective for Ser21/9-phosphorylated GSK-3 to determine whether the GSK-3 inhibitors can cause the inhibition of GSK-3 activity. As shown in Fig. 1F, treatment of cortical slices with LiCl (5 mM) or TDZD (2–10 μM) markedly increased the level of phosphorylated GSK-3α/β without changing the level of total

GSK-3α/β, indicating that the GSK-3 inhibitors indeed resulted in GSK-3 inactivation.

Next we tested whether the pharmacological agents we used converge on GSK-3 to regulate NMDA receptor current. To do so, we coapplied different GSK-3 inhibitors. As shown in Fig. 2A, after TDZD suppression of NMDAR current, subsequent addition of LiCl did not cause further reduction of NMDAR current. Likewise, combined application of TDZD with LiCl after sole application of LiCl did not have further effect on NMDAR current (Fig. 2B). As summarized in Fig. 2C, the percentage reduction of NMDAR current by coapplication of TDZD and LiCl was similar to that by TDZD alone or LiCl alone, suggesting that one GSK-3 inhibitor occludes the effect of another GSK-3 inhibitor.

Given the effect of GSK-3 inhibitors on NMDAR current, we would like to know what the normal stimulus is that could activate this pathway. Insulin has been found to induce GSK-3 inhibition via protein kinase B (also called AKT) signaling (Cohen and Frame, 2001). Thus, we examined the effect of insulin on NMDAR current. As shown in Fig. 2D, application of insulin (2 μM) caused a decrease of NMDAR current (17.5 $\pm$ 1.2%, $n = 22$, Fig. 2F) and occluded the effect of subsequently applied GSK-3 inhibitor SB216763 (Fig. 2E, 17.8 $\pm$ 2.2%, $n = 9$, Fig. 2F). The effect of TDZD on NMDAR current was also significantly attenuated in the presence of insulin ($n = 4$, data not shown). These results suggest that activation of insulin signaling could down-regulate whole-cell NMDAR current via inhibiting GSK-3.

Because the NMDA-evoked current in isolated neurons is mediated by both synaptic and extrasynaptic NMDA receptors, we further examined the effect of GSK-3 on NMDAR-EPSC evoked by stimulation of synaptic NMDA receptors in cortical slices. As shown in Fig. 3, A and B, application of TDZD (20 μM) induced a significant reduction in the amplitude of NMDAR-EPSC. In parallel control measurements in which no TDZD was administered, NMDAR-EPSC remained stable throughout the length of the recording. In a sample of cortical pyramidal neurons we examined, TDZD decreased the mean amplitude of NMDAR-EPSC by 30.2 $\pm$ 2.1% ($n = 10$, $p < 0.001$, Mann-Whitney).

Cellular Knockdown of GSK-3 Leads to Smaller NMDAR Current and Loss of Its Regulation by GSK-3 Inhibitors in Cultured Cortical Pyramidal Neurons. To further test the role of GSK-3 in the regulation of NMDA
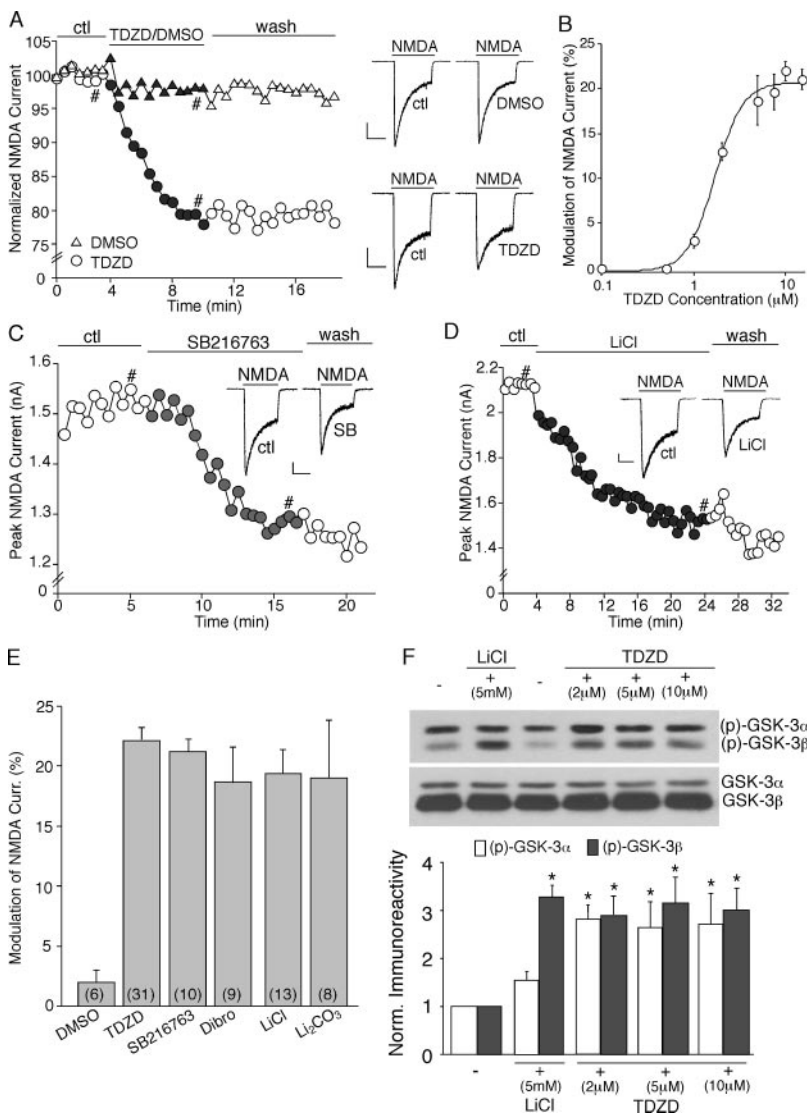

Fig. 1. GSK-3 inhibitors reduce NMDA receptor-mediated ionic current in dissociated cortical pyramidal neurons. A, C, and D, plot of peak NMDAR current showing that the selective GSK-3 inhibitors TDZD (10 μM; A), SB216763 (10 μM; C), LiCl (5 mM; D), but not the control vehicle DMSO (A), decreased NMDA (100 μM)-evoked current in acutely isolated neurons. Inset, representative current traces (at time points denoted by #). Scale bars, 250 pA, 1 s. B, dose-response data showing the percentage reduction of NMDAR current by different concentrations of TDZD. E, cumulative data (mean $\pm$ S.E.M.) showing the percentage reduction of NMDAR current by various GSK-3 inhibitors in freshly dissociated neurons. The number of cells tested in each condition is shown in each bar. F, representative Western blotting and quantitative analysis from four to six experiments showing the effect of LiCl (5 mM) or TDZD (2, 5, and 10 μM) on Ser21/9 phosphorylated GSK-3α/β and total GSK-3α/β in cortical slices. $*$, $p < 0.001$, ANOVA.
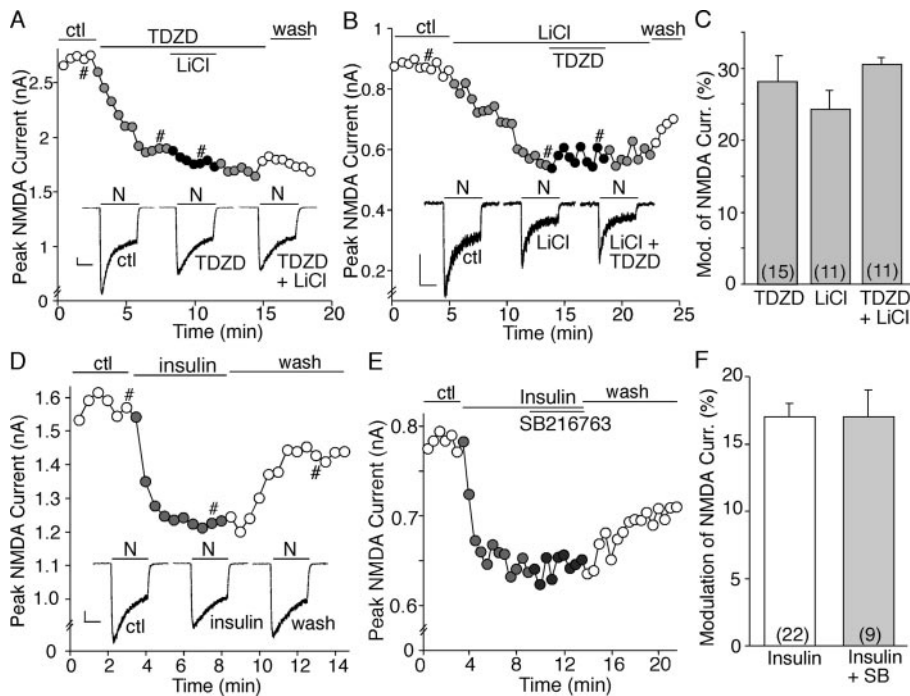
Fig. 2. The effects of different GSK-3 inhibitors on NMDAR current occlude each other and are mimicked and occluded by insulin application. A and B, plot of peak NMDAR current showing the effect of TDZD (10 μM) alone followed by coapplication of TDZD and LiCl (5 mM; A) or the effect of LiCl alone followed by coapplication of LiCl and TDZD (B) in representative neurons. C, cumulative data (mean ± S.E.M.) showing the percentage reduction of NMDAR current by individual or combined GSK-3 inhibitors. D and E, plot of peak NMDAR current showing the effect of insulin (2 μM; D) or insulin followed by coapplication of insulin and SB216763 (10 μM; E). Inset (A, B, and D), current traces (at time points denoted by #). Scale bars, 250 pA, 1 s. F, cumulative data (mean ± S.E.M.) showing the percentage reduction of NMDAR current by insulin or combined application of insulin and SB216763.

receptors, we suppressed GSK-3 protein expression in cultured cortical neurons (11 DIV) by transfecting an siRNA directed against GSK-3α or GSK-3β (Phiel et al., 2003). GFP was cotransfected with GSK-3 siRNA. In all of the GFP-positive neurons we observed, the GSK-3α/β siRNA caused efficient and specific down-regulation of GSK-3α/β expression (Fig. 4, A and B; GSK-3α, $n = 12$; GSK-3β, $n = 15$), which is likely to cause functional inactivation of GSK-3. So we examined NMDAR current in GSK-3 siRNA-transfected neurons. Control neurons were transfected with GFP alone or with a scrambled siRNA. As shown in Fig. 4C, in GSK-3β siRNA-transfected neurons, the distribution of NMDAR current density (in picoamperes per picofarads) was shifted to the left with smaller values compared with nontransfected neurons or neurons transfected with GFP alone or GSK-3α siRNA. Transfecting both GSK-3α and GSK-3β siRNAs also caused a leftward shift of the NMDAR current density. The average NMDAR current density (in picoamperes per picofarads) in neurons transfected with different agents is summarized in Fig. 4D. Significantly ($p < 0.001$, ANOVA) smaller values were found in neurons transfected with GSK-3β siRNA (16.3 ± 0.8, $n = 18$) or both GSK-3α and GSK-3β siRNAs (16.7 ± 1.1, $n = 19$) compared with nontransfected neurons (22.5 ± 1.0, $n = 12$), GFP-transfected neurons (23.1 ± 0.8, $n = 18$), scrambled siRNA-transfected neurons (20.8 ± 1.5, $n = 8$), or GSK-3α siRNA-transfected neurons (20.5 ± 0.9, $n = 15$). These results suggest that cellular knockdown of GSK-3β results in depressed basal NMDAR current.

We next examined the effect of GSK-3 inhibitors on NMDAR current in neurons transfected with GSK-3 siRNA. As shown in Fig. 4E, TDZD had little effect on NMDAR current in the GFP-positive neuron transfected with both GSK-3α and GSK-3β siRNAs, whereas it produced a potent reduction of NMDAR current in the control neuron transfected with GFP alone. As summarized in Fig. 4F, in cultured

neurons transfected with GSK-3α and GSK-3β siRNAs, TDZD reduced NMDAR currents by 6.0 ± 1.7% ($n = 11$, $p > 0.05$, Mann-Whitney), which was significantly ($p < 0.001$, ANOVA) smaller than the effect of TDZD in control neurons transfected with GFP alone (21.0 ± 1.1%, $n = 6$, $p < 0.001$, Mann-Whitney). These results indicate that suppression of GSK-3 expression prevents exogenously applied GSK-3 inhibitors from regulating NMDAR current.

The GSK-3 Regulation of NMDAR Current Is Not Dependent on the Kinesin Motor Protein or Cytoskeleton Stability. In the next series of experiments, we sought to determine the potential mechanism underlying the reduction of NMDAR current by GSK-3 inhibitors. In mature cortical synapses, the primary NMDA receptors are composed of NR1/NR2A or NR1/NR2B, which differ in subcellular localization. To determine which subpopulation(s) of NMDARs is
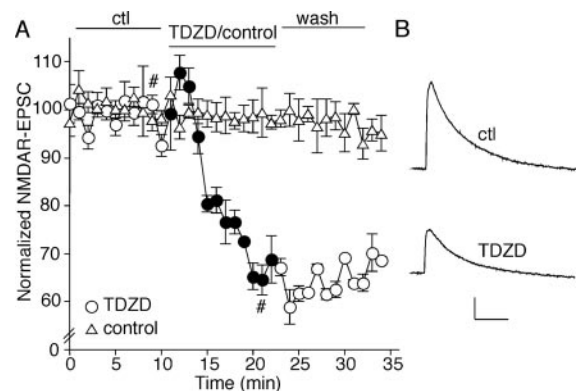

Fig. 3. GSK-3 inhibitors reduce NMDA receptor-mediated synaptic current in cortical slices. A, plot of normalized peak evoked NMDAR-EPSC as a function of time and TDZD (20 μM) application. Each point represents the average peak (mean ± S.E.M.) of three consecutive NMDAR-EPSCs. B, Representative current traces (average of 10 trials) taken from the records used to construct A (at time points denoted by #). Scale bars, 100 pA, 200 ms.

modulated by GSK-3, we applied the selective inhibitor of NR2B subunit, ifenprodil. As shown in Fig. 5A, in the presence of ifenprodil, TDZD had almost no effect on the remaining NMDAR current ($2.3 \pm 1.0\%$, $n = 19$), suggesting that GSK-3 primarily target NR2B subunit-containing NMDA receptors.

After NMDA receptors leave the endoplasmic reticulum, they are transported along microtubules in dendrites via the kinesin motor protein KIF17, which is linked to NR2B-containing vesicles (Setou et al., 2000). It has been found that GSK-3 phosphorylates kinesin light chains and causes the detachment of kinesin from transported cargoes, leading to a reduction in kinesin-based motility (Morfini et al., 2002). To test whether the KIF17-mediated transport of NMDA receptors is involved in the GSK-3 regulation of NMDAR current, we performed cellular knockdown of KIF17 by treatment of cortical cultures with antisense oligonucleotides and examined the effect of TDZD on NMDAR current in these cultures. Our previous studies have shown that KIF17 antisense oligonucleotides, but not sense oligonucleotides, totally inhibited KIF17-mediated functions (Yuen et al., 2005a,b). However, in KIF17 antisense ($1\ \mu M$)-treated neurons, TDZD had

an intact inhibitory effect on NMDAR current similar to what was found in neurons exposed to KIF17 sense oligonucleotides ($1\ \mu M$; Fig. 5, B and C). These results suggest that the GSK-3 modulation of NMDAR current does not involve the motor protein KIF17-based transport of NR2B-containing NMDA receptors.

GSK-3, by targeting different microtubule binding proteins, has been found to regulate several aspects of microtubule assembly, including microtubule dynamics, microtubule stability, and microtubule polymerization (Zhou and Snider, 2005). Our recent studies have shown that microtubule stability plays a role in controlling the trafficking and function of NMDA receptor channels in cortical pyramidal neurons (Yuen et al., 2005a,b). To test whether GSK-3 regulates NMDAR current by affecting microtubule assembly, we examined the effect of TDZD in the presence of agents that depolymerize or stabilize microtubules. As shown in Fig. 5D, application of the microtubule-depolymerizing agent nocodazole ($30\ \mu M$) suppressed NMDAR currents, but subsequent application of TDZD in the presence of nocodazole produced a further reducing effect on NMDAR current. On the other hand, dialysis with paclitaxel (Taxol; $40\ \mu M$), a microtubule-
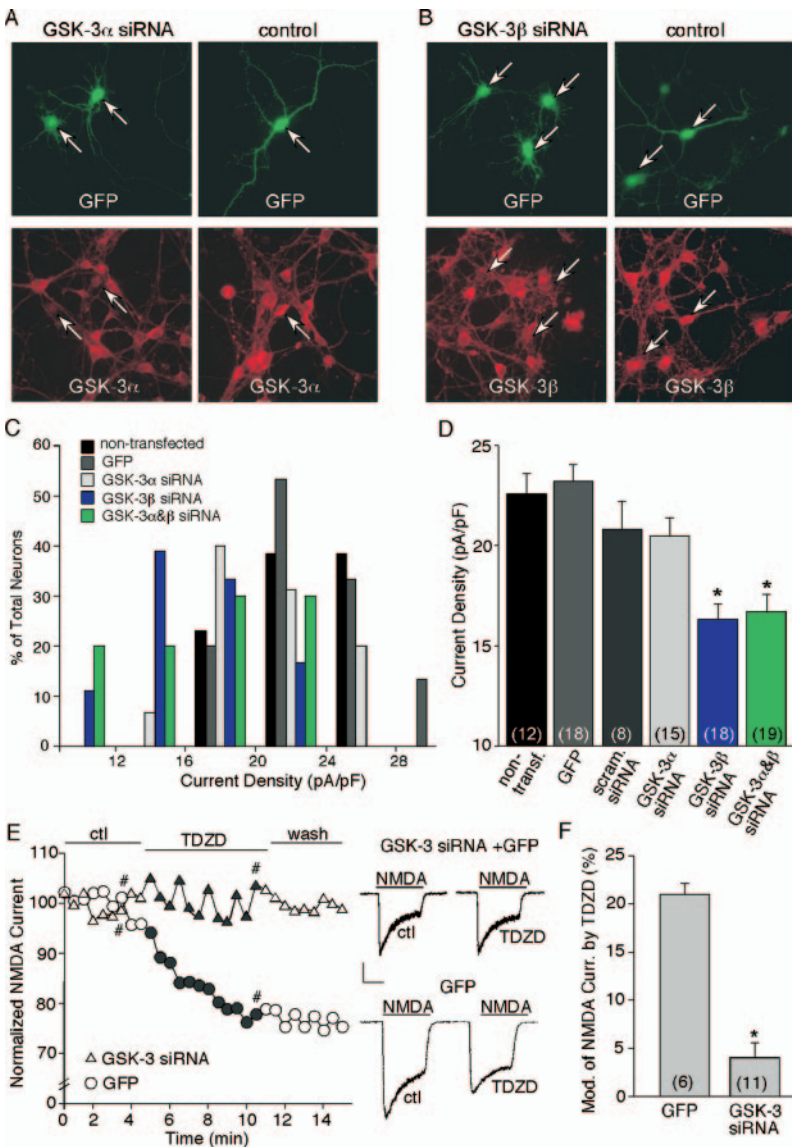

Fig. 4. Suppressing GSK-3 expression leads to smaller NMDAR current and loss of its regulation by GSK-3 inhibitors. A and B, representative immunocytochemical images stained with anti-GSK-3α (A) or anti-GSK-3β (B) in cultured cortical pyramidal neurons cotransfected with GFP and GSK-3α siRNA (A), GFP and GSK-3β siRNA (B), or transfected with GFP alone (control). Note that GSK-3α/β siRNA suppressed the expression of GSK-3α/β in GFP-positive neurons. C and D, Distribution (C) and cumulative average (D) of NMDAR current density (in picoamperes per picofarads) in cultured neurons transfected with GFP, scrambled siRNA, GSK-3α siRNA, GSK-3β siRNA, or both GSK-3α and GSK-3β siRNAs. *, $p < 0.001$, ANOVA. E, plot of peak NMDAR current showing the effect of TDZD (20 μM) in a GFP-positive neuron transfected with GSK-3α/β siRNA and a GFP-positive neuron without GSK-3 siRNA transfection. Inset, representative current traces (at time points denoted by #). Scale bars, 250 pA, 1 s. F, cumulative data (mean $\pm$ S.E.M.) showing the percentage reduction of NMDAR current by TDZD in a sample of GFP-positive neurons transfected with or without GSK-3α/β siRNA. *, $p < 0.001$, ANOVA.

stabilizing agent, failed to block the effect of TDZD on NMDAR current (Fig. 5E). As summarized in Fig. 5F, the modulation of NMDAR current by TDZD was not affected by microtubule depolymerizer nocodazole, by colchicine (30 μM), or by the microtubule stabilizer paclitaxel, suggesting the lack of involvement of microtubules in the GSK-3 regulation of NMDAR current.

A previous study has found that an inactive phosphorylated pool of GSK-3 colocalizes with F-actin in neurons and plays a key role in regulating axonal growth (Eickholt et al., 2002). To determine whether the GSK-3 modulation of NMDAR current is affected by the integrity of F-actin, we used the potent actin depolymerizing agent latrunculin B (Gu et al., 2005). As shown in Fig. 5G, application of latrunculin (5 μM) resulted in a gradual decrease of NMDAR current. Subsequent application of TDZD in the presence of latrunculin still induced a marked reduction of NMDAR current, indicating that latrunculin did not occlude the effect of TDZD. To further test the involvement of actin cytoskeleton, we dialyzed neurons with phalloidin (5 μM), an actin-stabilizing compound. As shown in Fig. 5H, the TDZD-induced reduction of NMDAR current was not prevented when actin filaments were stabilized by phalloidin (Gu et al., 2005). The unaltered effects of TDZD on NMDAR current in the presence of actin manipulating agents (Fig. 5I) suggest that the

GSK-3 regulation of NMDAR current is not dependent on actin filaments.

The GSK-3 Regulation of NMDAR Current Involves the Clathrin/Dynamin-Dependent Internalization of NMDA Receptors that Is Mediated by Rab5. To test whether clathrin-dependent endocytosis of NMDA receptors (Roche et al., 2001) is involved in the GSK-3 modulation of NMDAR current, we dialyzed neurons with a dynamin inhibitory peptide, QVPSRPNRAP, which interferes with the binding of amphiphysin with dynamin and therefore prevents endocytosis through clathrin-coated pits (Gout et al., 1993). We found that the effect of TDZD was largely abolished in neurons loaded with the dynamin inhibitory peptide (50 μM, Fig. 6, A and B; $4.0 \pm 1.2\%$, $n = 15$), compared with neurons loaded with a scrambled control peptide ($22.4 \pm 1.0\%$, $n = 10$). It suggests that the mechanism underlying the GSK-3 inhibitor-induced down-regulation of NMDAR current is a decrease of functional surface NMDA receptors mediated by clathrin/dynamin-dependent endocytosis.

Given the potential involvement of GSK-3 in NMDAR internalization, we further examined the role of Rab5, a key mediator of protein transport from plasma membrane to early endosomes during clathrin-dependent endocytosis (Bucci et al., 1992) in the GSK-3 regulation of NMDAR current. To do so, we injected neurons with the purified
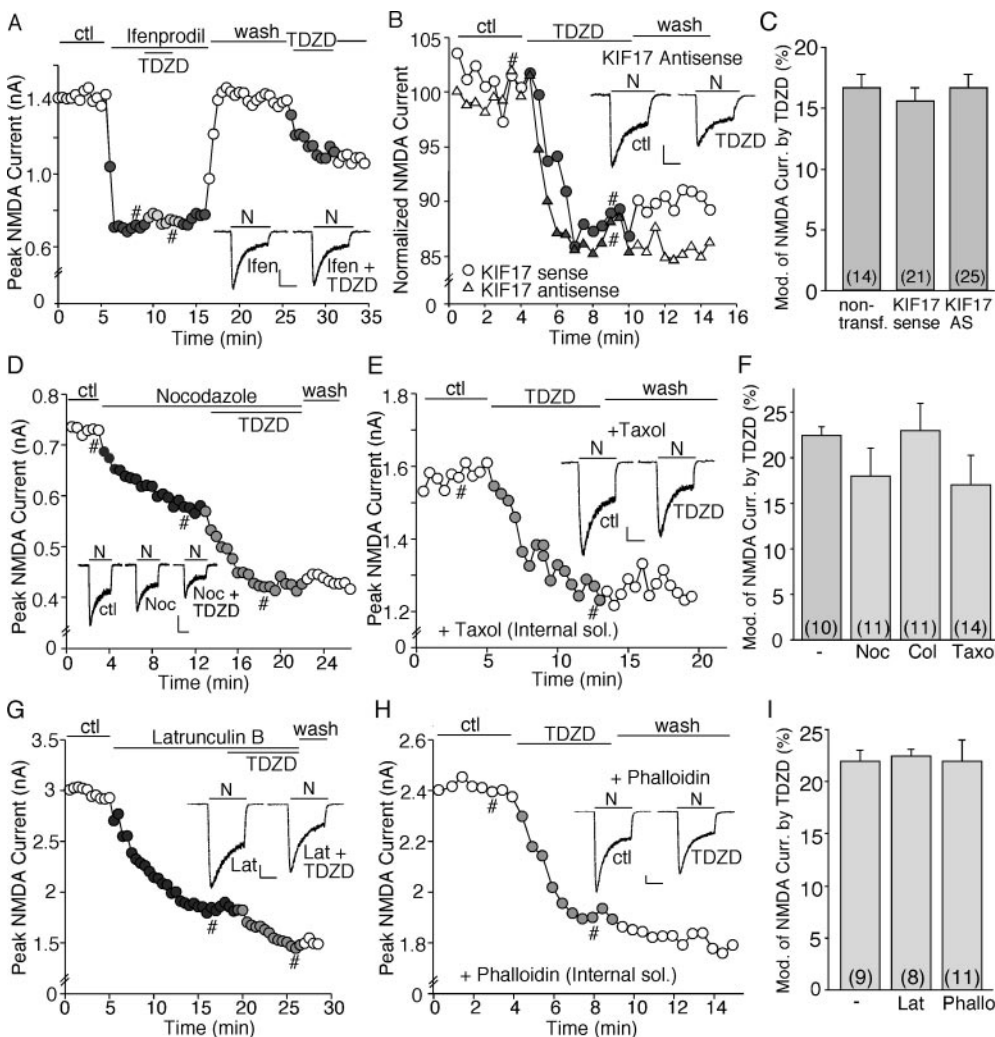

Fig. 5. GSK-3 regulation of NMDAR current is independent of KIF17-based transport of NR2B-containing vesicles, microtubule stability, or F-actin integrity. A, plot of peak NMDAR current showing that the effect of TDZD (10 μM) was abolished in the presence of ifenprodil (3 μM), the selective inhibitor of NR2B subunit. B, plot of peak NMDAR current showing the effect of TDZD in neurons treated with KIF17 antisense or sense oligonucleotides. C, cumulative data (mean $\pm$ S.E.M.) showing the percentage reduction of NMDAR current by TDZD in a sample of cultured neurons treated with KIF17 antisense or sense oligonucleotides. D and G, plots of peak NMDAR currents showing that the effect of TDZD (10 μM) was not occluded by the microtubule-depolymerizing agent nocodazole (30 μM; D) or the actin-depolymerizing agent latrunculin B (5 μM; G). E and H, plots of peak NMDAR currents showing that dialysis with the microtubule-stabilizing agent paclitaxel (40 μM; E) or the actin-stabilizing agent phalloidin (5 μM; H) did not block the effect of TDZD. Inset (A, B, D, E, G, and H), representative current traces (at time points denoted by #). Scale bars, 250 pA, 1 s. F and I, cumulative data (mean $\pm$ S.E.M.) showing the percentage reduction of NMDAR current by TDZD in the absence or presence of various agents that interfere with microtubule (F) or actin (I) network.

dominant-negative (DN) mutant form of Rab5 protein (Rab5S34N) or the purified constitutively active (CA) variant of Rab5 protein (Rab5Q79L), which inhibits or accelerates clathrin-mediated endocytosis, respectively (Stenmark et al., 1994). Whereas most endogenous Rab5 is associated with membrane compartments, it has been shown that recombinant wild-type Rab5 overexpressed in hippocampal slice cultures is also membrane-bound, but DN-Rab5 is predominantly cytosolic (Brown et al., 2005). We found that the effect of TDZD on NMDAR current was diminished in cells loaded with DN-Rab5 or CA-Rab5 (4 μg/ml, Fig. 6C). Likewise, another GSK-3 inhibitor, SB216763, also failed to regulate NMDAR current with the dialysis of DN-Rab5 (Fig. 6D). In a sample of neurons tested (Fig. 6E), the basal NMDAR current was significantly reduced with CA-Rab5 injection (580 $\pm$ 124 pA, $n = 5$) compared with control cells (1100 $\pm$ 90 pA, $n = 7$) or cells injected with DN-Rab5 (1005.5 $\pm$ 61.5 pA, $n = 9$). The effect of GSK-3 inhibitors on NMDAR current was mark-

edly blocked by DN-Rab5 (Fig. 6F; TDZD, 7.2 $\pm$ 1.1%, $n = 6$; SB216763, 3.0 $\pm$ 0.8%, $n = 10$) and was largely occluded by CA-Rab5 (TDZD, 8.0 $\pm$ 1.6%, $n = 8$). Moreover, loading cells with the Rab5 antibody (2 μg/ml), which binds to and inhibits Rab5, significantly blocked the effect of SB216763 on NMDAR current (Fig. 6F, 5.0 $\pm$ 1.1%, $n = 15$), whereas the heat-inactivated Rab5 antibody was ineffective (21.0 $\pm$ 2.1%, $n = 5$). These results suggest that Rab5 activity is required for the clathrin-dependent NMDAR internalization, which is regulated by GSK-3.

To provide more direct evidence showing that the GSK-3 regulation of NMDAR current can be accounted for by the altered number of NMDA receptors on the cell membrane, we first performed surface biotinylation experiments to measure levels of surface NR1 in cortical slices. Surface proteins were labeled with sulfo-NHS-LC-biotin, and then biotinylated surface proteins were separated from nonlabeled intracellular proteins by reaction with Neutravidin beads. Surface and
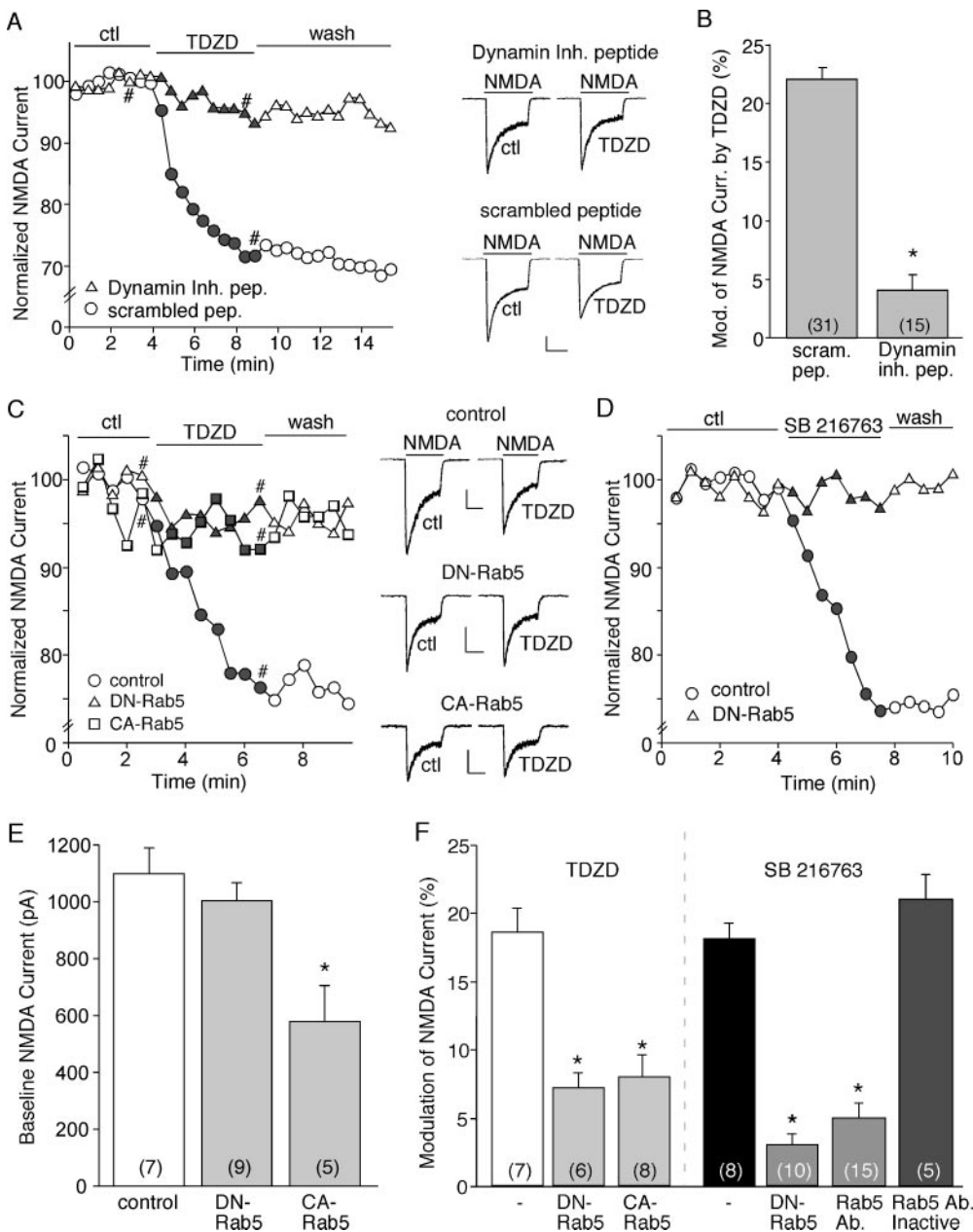

Fig. 6. GSK-3 regulation of NMDAR current involves the clathrin/dynamin-dependent endocytosis of NMDA receptors that is mediated by Rab5. A, plot of normalized peak NMDAR current as a function of time and TDZD (10 μM) application in neurons dialyzed with the dynamin inhibitory peptide (50 μM) or a scrambled control peptide (50 μM). B, cumulative data (mean $\pm$ S.E.M.) showing the percentage reduction of NMDAR current by TDZD in neurons injected with different peptides. $*$, $p < 0.001$, ANOVA. C and D, plot of normalized peak NMDAR current as a function of time and TDZD (10 μM; C) or SB216763 (10 μM; D) application in neurons dialyzed with the purified dominant-negative Rab5 (DN-Rab5, 4 μg/ml) or constitutively active Rab5 (CA-Rab5, 4 μg/ml) protein. Inset (A and C), representative current traces (at time points denoted by #). Scale bars, 250 pA, 1 s. E, cumulative data (mean $\pm$ S.E.M.) showing the amplitude of peak NMDAR current in neurons loaded with or without DN-Rab5 or CA-Rab5. $*$, $p < 0.005$, ANOVA. F, cumulative data (mean $\pm$ S.E.M.) showing the percentage reduction of NMDAR current by TDZD or SB216763 in neurons injected with different agents. $*$, $p < 0.001$, ANOVA.

total proteins were subjected to electrophoresis and probed with an antibody against the NR1 subunit. As shown in Fig. 7A, treatment of cortical slices with TDZD (10 μM, 10 min) reduced the level of surface NR1 with no change in the total NR1 protein. Furthermore, the TDZD effect on the surface expression of NR1 was blocked by pretreatment with the myristoylated (cell-permeable) dynamin inhibitory peptide (50 μM, 30 min). Quantitative analysis (Fig. 7B) in a sample of experiments indicated that TDZD decreased the level of surface NR1 to $58 \pm 6.8\%$ of control ($n = 8$; $p < 0.01$, ANOVA) but failed to do so in the presence of the dynamin inhibitory peptide ($95 \pm 4.5\%$ of control, $n = 3$; $p > 0.05$, ANOVA). Another GSK-3 inhibitor, SB216763 (10 μM, 15 min), also significantly decreased the level of surface NR1 ($54 \pm 3.9\%$ of control, $n = 4$; $p < 0.01$, ANOVA).

To further evaluate the changes of surface NMDAR subunits induced by GSK-3 inhibitors, we transfected neurons with GFP-tagged NR2B or NR2A (the GFP tag is placed at the extracellular N terminus of NR2), which has been shown to exhibit similar properties and localization as endogenous NR2B or NR2A subunit (Luo et al., 2002). The surface distribution of recombinant NR2B or NR2A was assessed by immunostaining with anti-GFP primary antibody followed by rhodamine-conjugated secondary antibody in nonpermeabilized conditions. As shown in Fig. 7C, punctate red fluorescence was clearly visible on dendritic branches of GFP-NR2B-transfected cells under control conditions, whereas in neurons treated with SB216763 (10 μM, 10 min) or TDZD (10 μM, 10 min), the fluorescent GFP-NR2B surface clusters on

dendrites were significantly reduced (control, 65.6 ± 11.3 clusters/50 μm dendrites; SB216763, 44.1 ± 8.4 clusters/50 μm dendrites; TDZD, 40.3 ± 8.9 clusters/50 μm dendrites; $p < 0.01$, ANOVA, compared with control). In contrast, GFP-NR2A surface clusters on dendrites were not significantly affected by GSK-3 inhibitors (Fig. 7D; control, 58.8 ± 10.7 clusters/50 μm dendrites; SB216763, 55.6 ± 9.1 clusters/50 μm dendrites; TDZD, 53.3 ± 9.5 clusters/50 μm dendrites; $p > 0.05$, ANOVA, compared with control). The total amount of NR2B or NR2A (GFP channel) was not altered by GSK-3 inhibitor treatment (data not shown). Taken together, these results have demonstrated the involvement of GSK-3 in regulating NMDAR internalization.

GSK-3 Regulates the Clathrin-Dependent NMDAR Internalization that Is Affected by the Scaffolding Protein PSD-95. Because the clathrin-dependent internalization of NMDARs is prevented by the postsynaptic scaffolding protein PSD-95 (Roche et al., 2001), we further examined the involvement of PSD-95 in GSK-3 regulation of NMDARs. As shown in Fig. 8, A and B, SB216763 or TDZD treatment caused a significant reduction of NR1 that bound to PSD-95 (SB216763, $44.7 \pm 8.3\%$ of control, $n = 6$; TDZD, $40.8 \pm 7.5\%$ of control, $n = 6$; $p < 0.01$, ANOVA). The decreased association between NR1 and PSD-95 is consistent with the increased NMDAR internalization in response to GSK-3 inhibitors.

Next, we dialyzed neurons with a peptide derived from the NR2B C-terminal nine residues, NR2B9c, which contains the binding region for PSD-95 and has the capability to disrupt
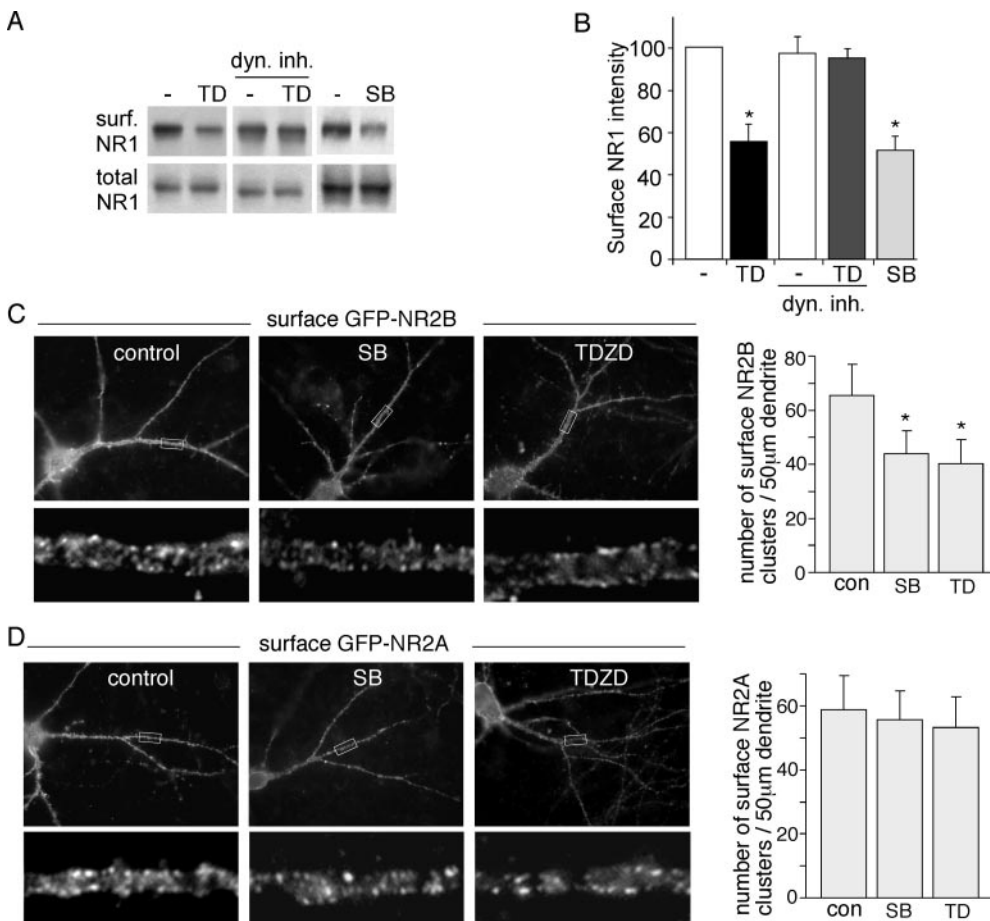

Fig. 7. GSK-3 inhibitors reduce surface NMDA receptors in a clathrin/dynamin-dependent mechanism. A, immunoblots showing the surface NR1 subunit and total NR1 subunit in cortical slices treated with TDZD (TD; 10 μM, 10 min) in the absence or presence of the membrane-permeable dynamin inhibitory peptide (50 μM, 30-min pretreatment) or cortical slices treated with SB216763 (SB; 10 μM, 15 min). B, quantitation of the surface NR1 subunit expression with various treatments. ∗, $p < 0.01$, ANOVA. C and D, left, immunocytochemical images of surface GFP-NR2B (C) or GFP-NR2A (D) in transfected cortical cultures either untreated (control) or treated with SB216763 (10 μM, 10 min) or TDZD (10 μM, 10 min). Enlarged versions of the boxed regions of dendrites are shown beneath each of the images. Right, quantitation of the density of surface GFP-NR2B (C) or GFP-NR2A (D) clusters on neuronal dendrites with various treatments. ∗, $p < 0.01$, ANOVA.

preformed NR2B-PSD-95 complexes (Aarts et al., 2002). As shown in Fig. 8, C and D, injection with the NR2B9c peptide (5 μM) caused a gradual decrease of NMDAR current (23 $\pm$ 3.3%, n = 10) and occluded the effect of subsequently applied GSK-3 inhibitor SB216763 (NR2B9c peptide + SB216763, 25 $\pm$ 1.5%, n = 8). In contrast, a scrambled control peptide (5 μM) had little effect on basal NMDAR current and failed to alter the effect of SB216763 (25 $\pm$ 1.3%, n = 6). Dialysis with low concentrations of NR2B9c peptide (1 μM or 100 nM) did not affect the basal NMDAR current or GSK-3 regulation (data not shown), suggesting that high concentrations of NR2B9c peptide (5 or 10 μM) are needed to perturb the association between NMDA receptors and PSD-95. Taken together, these results indicate that inhibiting GSK-3 increases the clathrin-dependent NMDAR internalization, which is affected by the level of PSD-95-bound NMDA receptors.

Discussion

Discovered originally as a protein involved in regulating the glucose level in skeletal muscle cells, GSK-3 is also expressed at a very high level in the central nervous system. On one hand, this distribution pattern might be related to the brain's high demand of glucose as its primary energy source. The high level of GSK-3 could prevent glycogen synthesis and therefore maintain glucose molecules in the accessible form. On the other hand, the high level of GSK-3 in central nervous system also suggests that it may be critically involved in

Fig. 8. The association between NMDA receptors and PSD-95 is involved in GSK-3 regulation of NMDAR current. A, effect of GSK-3 inhibitors on the interaction of NMDA receptors with PSD-95. Cell lysates from cortical slices were incubated with TDZD (10 μM, 10 min) or SB216763 (10 μM, 15 min) followed by immunoprecipitation with anti-NR1 antibody and Western blot analysis for PSD-95. Note that a control IgG resulted in no signal in the coimmunoprecipitation experiments. B, bar graphs showing the level of NR1 bound to PSD-95 in the absence or presence of GSK-3 inhibitors. ∗, p < 0.01, ANOVA. C, plot of normalized peak NMDAR current as a function of time and SB216763 (10 μM) application in neurons dialyzed with the NR2B9c peptide (5 μM) or a scrambled control peptide (5 μM). D, cumulative data (mean $\pm$ S.E.M.) showing the percentage reduction of NMDAR current by different peptides without or with subsequently added SB216763. ∗, p < 0.001, ANOVA.

regulating neural physiological processes. GSK-3 is known to play important roles in the cell fate and differentiation, cellular architecture and motility, cell survival and apoptotic signaling, and is related to the pathogenesis of a diverse array of diseases (Welsh et al., 1996; Jope and Johnson, 2004). In particular, GSK-3 has been implicated in AD because it is associated with the production of Aβ (Phiel et al., 2003) and hyperphosphorylated τ protein (Hong et al., 1997), both of which are prominent features of AD. In this study, we found that the whole-cell NMDAR current was reduced in the presence of various GSK-3 inhibitors. Additional evidence is obtained when the cellular GSK-3β protein is specifically knocked down by an siRNA, in which the basal NMDAR current density is smaller and the modulatory effect of GSK-3 inhibitors is abolished. Because GSK-3β knockdown alone is sufficient to down-regulate NMDAR current, it suggests that constitutively active endogenous GSK-3β is playing an important role in maintaining the expression of functional NMDARs on the surface of cortical neurons under basal conditions. Given the key role of NMDARs in synaptic plasticity, our data indicate that inactivating GSK-3 will have direct impact on synaptic functions, which provides a new mechanism underlying the role of GSK-3 in AD, a disease linked to synaptic failure (Selkoe, 2002).

Emerging evidence suggests that NMDAR trafficking involves multiple steps that are tightly regulated, including exiting from endoplasmic reticulum, transporting along microtubules on dendrites by the kinesin motor protein KIF17, delivery to actin-enriched postsynaptic density, internalization from the cell surface, and lateral diffusion at synaptic and extrasynaptic sites in the plasma membrane (Wenthold et al., 2003). The abilities of GSK-3 to regulate microtubule dynamics (Zhou and Snider, 2005) and unload vesicles from kinesin protein family (Morfini et al., 2002) make it a good candidate potentially involved in the microtubule/KIF17-based transport of NMDARs (Yuen et al., 2005b). However, our data with microtubule-manipulating agents and KIF17 antisense oligonucleotides suggest that GSK-3 is not regulating NMDAR trafficking through interference with NMDAR transport along dendritic microtubules. Moreover, actin-manipulating agents also fail to affect GSK-3 regulation of NMDAR channels.

Inactivating GSK-3 has been shown to promote the recycling of internalized integrins through an unclear mechanism (Roberts et al., 2004). To test the possible involvement of GSK-3 in regulating NMDAR internalization, we examined the effect of GSK-3 inhibitors on the clathrin-mediated endocytosis of NMDARs, which is by far the most prevalent form of regulated endocytosis. In the presence of a dynamin inhibitory peptide to prevent endocytosis through clathrin-coated pits (Gout et al., 1993), GSK-3 inhibitors fail to regulate NMDAR current, which supports the role of GSK-3 in NMDAR internalization. The involvement of GSK-3 in the clathrin/dynamin-dependent NMDAR internalization is further demonstrated in the series of experiments with Rab5. Rab5, a member of the Rab family of small GTPases that function as specific regulators of vesicle transport between organelles (Zerial and McBride, 2001), is a key coordinator of early endocytic trafficking events, including early endosome fusion, internalization, and clathrin-coated vesicle formation. Dominant-negative Rab5 blocks the effect of GSK-3 inhibitors on NMDAR current, whereas constitutively active Rab5
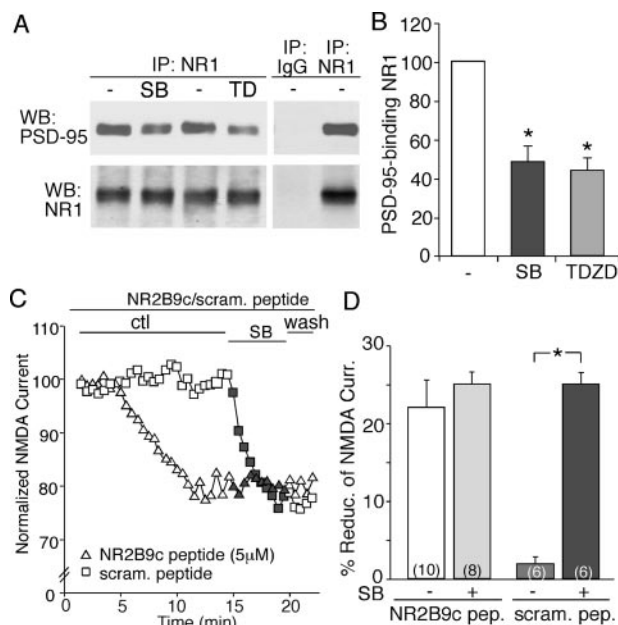
decreases basal NMDAR current and occludes the effect of GSK-3 inhibitors, suggesting that GSK-3 regulates NMDAR current via affecting Rab5/clathrin-mediated NMDAR internalization. More direct evidence comes from biochemical and immunocytochemical studies. In response to GSK-3 inhibitor treatment, cortical neurons show a markedly reduced level of surface NR1 and NR2B and significantly increased level of internalized NR1 and NR2B. In contrast, GSK-3 inhibitors do not have a significant effect on surface NR2A clusters, consistent with the electrophysiological finding that NR2B-containing NMDARs are the major target of GSK-3.

The regulatory pathway underlying the endocytosis of different NMDAR subunits is quite complex. Previous studies have found that extrasynaptic NMDARs (NR2B-predominated) have a higher rate of use-dependent turnover from the surface than synaptic NMDARs (NR2A-predominated), presumably resulting from an altered balance in their interactions with tyrosine kinases/phosphatases, and/or lack of interaction with PDZ proteins (Li et al., 2002). It has been shown consistently that NR2A and NR2B have distinct endocytic motifs and endocytic sorting, with NR2B undergoing more robust endocytosis than NR2A in mature cultures (Lavezzari et al., 2004). Thus, the lack of GSK-3 effect on NR2A may be caused by the lack of very active endocytosis of NR2A in native cortical neurons.

The anchoring protein PSD-95 has been found to affect NMDAR internalization (Roche et al., 2001). An AP-2 binding motif (YEKL) located on the distal C terminus of NR2B is normally covered up by PSD-95 to prevent internalization (Roche et al., 2001). PDZ protein-mediated stabilization and AP-2-mediated internalization actually control the synaptic localization of NR2B-containing NMDA receptors (Prybylowski et al., 2005). Because GSK-3 regulates NMDAR internalization, we further examined the involvement of PSD-95. Biochemical evidence indicates that the association of NMDARs with PSD-95 is reduced in response to GSK-3 inhibitors. Moreover, electrophysiological data demonstrate that perturbing NR2-PSD-95 complexes causes a gradual decrease of NMDAR current and occludes the effect of subsequently applied GSK-3 inhibitors. Hence, constitutively active GSK-3 is important for stabilizing and/or promoting the expression of surface NMDARs that is affected by the binding between PSD-95 and NMDARs.

The mechanism underlying how GSK-3 inhibitors regulate NMDAR internalization depends on what protein(s) is actually targeted by GSK-3. One possibility is that the dynamin-like protein, a putative GSK-3 substrate (Chen et al., 2000), is the target of GSK-3 inhibitors in the regulation of NMDA receptors. This possibility is supported by the finding that GSK-3 represents a potent and unique clathrin-coated vesicle-associated protein kinase (Yu and Yang, 1993). Another possibility is that the putative GSK-3 substrate protein phosphatase 1 (Jope and Johnson, 2004), which participates in the regulation of the association and dissociation cycle of the clathrin-based endocytic machinery (Slepnev et al., 1998), is a potential target of GSK-3 involved in its regulation of NR2B/AP-2 interactions and the ensuing NMDAR internalization.

A recent study shows that stimulation of NR2B-containing NMDA receptor disinhibits GSK-3 by protein phosphatase 1-mediated dephosphorylation of GSK-3 (Szatmari et al., 2005). Our present study indicates that GSK-3 inhibition leads to the suppression of NR2B function. Therefore, it provides a potential

mechanism for the protective role of GSK-3 inhibitors against the excessive activation of NR2B-GSK-3 loop and NMDAR-mediated excitotoxicity (Facci et al., 2003). Because pharmacological inhibitors of GSK-3 potentially could be used to treat several diseases, including AD and bipolar affective disorder (Meijer et al., 2004), our results provide an important framework to understand their actions on key targets involved in these diseases, such as NMDAR channels.

References

Aarts M, Liu Y, Liu L, Besshoh S, Arundine M, Gurd JW, Wang YT, Salter MW, and Tymianski M (2002) Treatment of ischemic brain damage by perturbing NMDA receptor- PSD-95 protein interactions. *Science* **298:**846–850.

Beaulieu JM, Sotnikova TD, Yao WD, Kockeritz L, Woodgett JR, Gainetdinov RR, and Caron MG (2004) Lithium antagonizes dopamine-dependent behaviors mediated by an AKT/glycogen synthase kinase 3 signaling cascade. *Proc Natl Acad Sci U S A* **101:**5099–5104.

Brown TC, Tran IC, Backos DS, and Esteban JA (2005) NMDA receptor-dependent activation of the small GTPase Rab5 drives the removal of synaptic AMPA receptors during hippocampal LTD. *Neuron* **45:**81–94.

Bucci C, Parton RG, Mather IH, Stunnenberg H, Simons K, Hoflack B, and Zerial M (1992) The small GTPase rab5 functions as a regulatory factor in the early endocytic pathway. *Cell* **70:**715–728.

Chen CH, Hwang SL, Howng SL, Chou CK, and Hong YR (2000) Three rat brain alternative splicing dynamin-like protein variants: interaction with the glycogen synthase kinase 3beta and action as a substrate. *Biochem Biophys Res Commun* **268:**893–898.

Cohen P and Frame S (2001) The renaissance of GSK3. *Nat Rev Mol Cell Biol* **2:**769–776.

Coyle JT and Duman RS (2003) Finding the intracellular signaling pathways affected by mood disorder treatments. *Neuron* **38:**157–160.

Cross DA, Alessi DR, Cohen P, Andjelkovich M, and Hemmings BA (1995) Inhibition of glycogen synthase kinase-3 by insulin mediated by protein kinase B. *Nature* **378:**785–789.

Doble BW and Woodgett JR (2003) GSK-3: tricks of the trade for a multi-tasking kinase. *J Cell Sci* **116:**1175–1186.

Eickholt BJ, Walsh FS, and Doherty P (2002) An inactive pool of GSK-3 at the leading edge of growth cones is implicated in Semaphorin 3A signaling. *J Cell Biol* **157:**211–217.

Emamian ES, Hall D, Birnbaum MJ, Karayiorgou M, and Gogos JA (2004) Convergent evidence for impaired AKT1-GSK3beta signaling in schizophrenia. *Nat Genet* **36:**131–137.

Facci L, Stevens DA, and Skaper SD (2003) Glycogen synthase kinase-3 inhibitors protect central neurons against excitotoxicity. *Neuroreport* **14:**1467–1470.

Frame S and Cohen P (2001) GSK3 takes center stage more than 20 years after its discovery. *Biochem J* **359:**1–16.

Gout I, Dhand R, Hiles ID, Fry MJ, Panayotou G, Das P, Truong O, Totty NF, Hsuan J, and Booker GW (1993) The GTPase dynamin binds to and is activated by a subset of SH3 domains. *Cell* **75:**25–36.

Gu Zu, Jiang Q, Fu AKY, Ip NY, and Yan Z (2005) Regulation of NMDA receptors by neuregulin signaling in prefrontal cortex. *J Neurosci* **25:**4974–4984.

Hong M, Chen DC, Klein PS, and Lee VM (1997) Lithium reduces tau phosphorylation by inhibition of glycogen synthase kinase-3. *J Biol Chem* **272:**25326–25332.

Jope RS and Johnson GV (2004) The glamour and gloom of glycogen synthase kinase-3. *Trends Biochem Sci* **29:**95–102.

Lavezzari G, McCallum J, Dewey CM, and Roche KW (2004) Subunit-specific regulation of NMDA receptor endocytosis. *J Neurosci* **24:**6383–6391.

Li B, Chen N, Luo T, Otsu Y, Murphy TH, and Raymond LA (2002) Differential regulation of synaptic and extra-synaptic NMDA receptors. *Nat Neurosci* **5:**833–834.

Luo JH, Fu ZY, Losi G, Kim BG, Prybylowski K, Vissel B, and Vicini S (2002) Functional expression of distinct NMDA channel subunits tagged with green fluorescent protein in hippocampal neurons in culture. *Neuropharmacology* **42:** 306–318.

Meijer L, Flajolet M, and Greengard P (2004) Pharmacological inhibitors of glycogen synthase kinase 3. *Trends Pharmacol Sci* **25:**471–480.

Morfini G, Szebenyi G, Elluru R, Ratner N, and Brady ST (2002) Glycogen synthase kinase 3 phosphorylates kinesin light chains and negatively regulates kinesin-based motility. *EMBO J* **21:**281–293.

Phiel CJ and Klein PS (2001) Molecular targets of lithium action. *Annu Rev Pharmacol Toxicol* **41:**789–813.

Phiel CJ, Wilson CA, Lee VM, and Klein PS (2003) GSK-3alpha regulates production of Alzheimer's disease amyloid-beta peptides. *Nature* **423:**435–439.

Prybylowski K, Chang K, Sans N, Kan L, Vicini S, and Wenthold RJ (2005) The synaptic localization of NR2B-containing NMDA receptors is controlled by interactions with PDZ proteins and AP-2. *Neuron* **47:**845–857.

Roberts MS, Woods AJ, Dale TC, Van Der Sluijs P, and Norman JC (2004) Protein kinase B/Akt acts via glycogen synthase kinase 3 to regulate recycling of alpha v beta 3 and alpha 5 beta 1 integrins. *Mol Cell Biol* **24:**1505–1515.

Roche KW, Standley S, McCallum J, Dune Ly C, Ehlers MD, and Wenthold RJ (2001) Molecular determinants of NMDA receptor internalization. *Nat Neurosci* **4:**794–802.

Selkoe DJ (2002) Alzheimer's disease is a synaptic failure. *Science* **298:**789–791.

Setou M, Nakagawa T, Seog DH, and Hirokawa N (2000) Kinesin superfamily motor protein KIF17 and mLin-10 in NMDA receptor-containing vesicle transport. *Science* **288:**1796–1802.

Slepnev VI, Ochoa GC, Butler MH, Grabs D, and De Camilli P (1998) Role of phosphorylation in regulation of the assembly of endocytic coat complexes. *Science* **281:**821–824.

Stenmark H, Parton RG, Steele-Mortimer O, Lutcke A, Gruenberg J, and Zerial M (1994) Inhibition of rab5 GTPase activity stimulates membrane fusion in endocytosis. *EMBO J* **13:**1287–1296.

Szatmari E, Habas A, Yang P, Zheng JJ, Hagg T, and Hetman M (2005) A positive feedback loop between glycogen synthase kinase 3β and protein phosphatase 1 after stimulation of NR2B NMDA receptors in forebrain neurons. *J Biol Chem* **280:**37526–37535.

Tsai G and Coyle JT (2002) Glutamatergic mechanisms in schizophrenia. *Annu Rev Pharmacol Toxicol* **42:**165–179.

Wang X, Zhong P, Gu Z, and Yan Z (2003) Regulation of NMDA receptors by dopamine D4 signaling in prefrontal cortex. *J Neurosci* **23:**9852–9861.

Welsh GI, Wilson C, and Proud CG (1996) GSK3: a SHAGGY frog story. *Trends Cell Biol* **6:**274–279.

Wenthold RJ, Prybylowski K, Standley S, Sans N, and Petralia RS (2003) Trafficking of NMDA receptors. *Annu Rev Pharmacol Toxicol* **43:**335–358.

Yu JS and Yang SD (1993) Identification and characterization of protein kinase FA/glycogen synthase kinase 3 in clathrin-coated brain vesicles. *J Neurochem* **60:**1714–1721.

Yuen EY, Jiang Q, Chen P, Gu Z, Feng J, and Yan Z (2005a) Serotonin 5-HT1A receptors regulate NMDA receptor channels through a microtubule-dependent mechanism. *J Neurosci* **25:**5488–5501.

Yuen EY, Jiang Q, Feng J, and Yan Z (2005b) Microtubule regulation of *N*-methyl-D-aspartate receptor channels in neurons. *J Biol Chem* **280:**29420–29427.

Zerial M and McBride H (2001) Rab proteins as membrane organizers. *Nat Rev Mol Cell Biol* **2:**107–117.

Zhou FQ and Snider WD (2005) GSK-3beta and microtubule assembly in axons. *Science* **308:**211–214.

Address correspondence to: Dr. Zhen Yan, Department of Physiology and Biophysics, State University of New York at Buffalo, 124 Sherman Hall, Buffalo, NY 14214. E-mail: zhenyan@buffalo.edu